 doi:10.20944/preprints202107.0318.v1

Article

Comment on the determination of the polar anchoring energy by capacitance measurements in nematic liquid crystals

Patrick Oswald

Univ Lyon, Ens de Lyon, Univ Claude Bernard, CNRS, Laboratoire de Physique, F-69342 Lyon, France.
* Correspondence: patrick.oswald@ens-lyon.fr

Abstract: Capacitance measurements have been extensively used to measure the anchoring extrapolation length L at a nematic-substrate interface. These measurements are extremely delicate because the value found for L often critically depends on the sample thickness and the voltage range chosen to perform the measurements. Several reasons have been proposed to explain this observation, such as the presence of inhomogeneities in the director distribution on the bounding plates or the variation with the electric field of the dielectric constants. In this paper I propose a new method to measure L_p that takes into account this second effect. This method is more general than that proposed in Murauski *et al.* Phys. Rev. E 71, 061707 (2005) because it does not assume that the anchoring angle is small and that the anchoring energy is of the Rapini-Papoular form. This method is applied to a cell of 8CB treated for planar unidirectional anchoring by photoalignment with the azobenzene dye Brilliant Yellow. The role of flexoelectric effects and the shape of the anchoring potential are discussed.

Keywords: nematic liquid crystal; anchoring energy; capacitance measurements; Freedericksz transition

1. Introduction

Measuring the anchoring energy W of the director at the bounding plates of a nematic cell is necessary to predict its electrooptical properties under electric field. This is important for basic physics to better understand the anchoring phenomena [1–3] and for the applications to electro-optic devices such as LCD displays to improve their performance [4]. In this paper, I focus more specifically on the measurement of the polar anchoring energy in planar cells filled with a liquid crystal (LC) of positive dielectric anisotropy. This measurement is very classical, but nonetheless extremely delicate as one immediately realizes after reading the literature on this subject. Indeed, the value of W obtained with the same LC and the same substates may differ by several orders of magnitude when measured by different groups [5]. In practice, various techniques have been proposed to measure W. Some of them analyze the deformation of the director field in the presence of a wall [6] or in a wedge cell [7–9]. Other use light scattering [10–12]. But the most widely used techniques are based on the action of an external field. Among them one can cite all-optical methods using magnetic or electric field as the ones described by Subacius *et al.* [13] or Murauski *et al.* [14] and much more standard methods using an electric field and capacitance and/or optical retardation measurements. In this last category, the method proposed by Yokoyama and van Sprang [15] at high electric field (YvS method) is certainly the most popular. This method consists of plotting R/R_0 as a function of $1/CV$. Here V is the applied voltage, C is the capacitance, R is the optical retardation between the ordinary and extraordinary rays (with the index 0 denoting that the measurement has been performed without electric field). The model predicts that in a certain range of voltage, $V_{\min} < V < V_{\max}$, the curve must be a line whose intersection with the ordinate axis gives W. The first inequality with $V_{\min} \approx 6V_c$, where V_c is the Fredericksz voltage, ensures that the tilt angle ϕ_m in the middle of the cell is equal to $\pi/2$ to better than 10^{-3} rad. The second inequality ensures that the tilt angle on the plates θ remains small enough in order that the actual anchoring potential is approximately given by the Rapini-Rapoular formula $W(\theta) = \frac{1}{2}W\sin^2\theta$ [16]. By assuming that it is the case for $\theta < 0.2$ rad, the calculation shows

Preprints (www.preprints.org) | NOT PEER-REVIEWED | Posted: 14 July 2021 doi:10.20944/preprints202107.0318.v1

that $V_{\max} \approx \frac{0.2}{\pi}\sqrt{\frac{\varepsilon_\perp}{\varepsilon_\parallel}}\frac{d}{L}V_c$ [17]. In practice, Nastishin *et al.* have shown that similar results can be obtained by just measuring the optical retardation in the same range of voltage (RV method) [5,17]. This method is interesting because it allows a local measurement of L. The problem with these two methods is that they often give very different values of L depending on the voltage interval (V_1, V_2) chosen to perform the fit of the experimental data, and this, even when $(V_1, V_2) \in (V_{\min}, V_{\max})$. Unphysical negative value of W_a can even be obtained [17]. According to Nastishin *et al.* [17] this unexpected behavior could be due to in-plane inhomogeneities of the cell (such as variations of the anchoring energy, easy axis, fractures in the patterned electrodes, etc.) thus making these methods difficult to use to determine a reliable value of W.

In this paper, I propose an alternative method to measure the polar (zenithal) anchoring energy W in a planar cell based on capacitance measurements at high electric field. The main difference with previous works is that I take into account the variation with the electric field of the dielectric constant $\varepsilon_\parallel$ and I use the full integral equations to fit the experimental data. In this way, the limitation to small tilt angles on the plates is waived and any form of the anchoring potential can be used. I will show that these improvements are necessary to obtain consistent results when the measurements are performed in thin samples under high electric field. The experiments will be performed by using the LC 8CB (4-octyl-4'-cyanobiphenyl) and the azo-dye Brilliant Yellow to treat the electrodes for planar unidirectional anchoring by photoalignment [18–20]. With this treatment, there is no pretilt angle at the electrodes which simplifies the problem.

2. Basic equations

I consider a planar sample. The x-axis is taken parallel to the anchoring direction on the electrodes and the z-axis is perpendicular to the electrodes, with $z = 0$ at the bottom electrode and $z = d$ at the top electrode. I denote by $\phi(z)$ the tilt angle of the director with respect to the x-axis and by θ the tilt angle on the electrodes ($\theta = \phi(0) = \phi(d)$). I suppose that there is no pretilt angle, which means that $\theta = 0$ when no electric field is applied. For now, the anchoring potential is assumed to be of the Rapini-Papoular form [16]

$$W(\theta) = \frac{1}{2}W\sin^2\theta \tag{1}$$

and I neglect the flexoelectric effect. When an electric field is applied and the anchoring is very strong the sample destabilizes above the Fredericksz critical voltage V_c given by [1,21]

$$V_c = \pi\sqrt{K_1/\varepsilon_0\varepsilon_a} \tag{2}$$

In this equation, ε_0 is the vacuum permittivity, $\varepsilon_a = \varepsilon_\parallel - \varepsilon_\perp$ is the dielectric anisotropy of the nematic phase and K_1 is the splay constant. The actual critical voltage V_c' is slightly smaller if the anchoring energy is taken into account and is solution of the following equation [1,16]:

$$\frac{d}{L} = \pi\frac{V_c'}{V_c}\tan\left(\frac{\pi V_c'}{2V_c}\right) \tag{3}$$

where $L = K_1/W$ is the anchoring extrapolation length. This equation shows that the ratio d/L must be larger than ≈ 200 in order that $V_c' \approx V_c$ to better than 1%.

The formulas that give the capacitance as a function of the applied voltage are well known [22,23] and are recalled in Ref. [24]. They considerably simplify at large voltage, when the maximum tilt angle ϕ_m in the middle of the cell is very close to $\pi/2$. Numerical calculations show that this condition is satisfied when $V \gtrsim 6V_c$, typically. In this limit, $\phi_m \approx \pi/2$ to better than 10^{-3} rad [5]. If the flexoelectric effects are screened out by the ions

Preprints (www.preprints.org) | NOT PEER-REVIEWED | Posted: 14 July 2021 doi:10.20944/preprints202107.0318.v1

contained in the LC – and this is usually the case experimentally– the capacitance can be calculated by using the formula [25]:

$$\frac{C}{C_\perp} = 1+\gamma - \frac{2}{\pi}\gamma\sqrt{1+\gamma}\frac{V_c}{V}\int_{\sin\theta}^{1}\sqrt{\frac{1+\kappa x^2}{1+\gamma x^2}}\mathrm{d}x \tag{4}$$

where $\gamma = \varepsilon_\parallel/\varepsilon_\perp - 1$ and $\kappa = K_3/K_1 - 1$ (with K_3 the bend constant) and $C_\perp = \varepsilon_0\varepsilon_\perp S/d$ is the capacitance measured below the onset of instability (with S the surface area of the electrodes).

The surface angle θ is obtained by solving the surface torque equation which reads by using the Rapini-Papoular potential [26]:

$$\sin\theta = \sqrt{\frac{1+\kappa\sin^2\theta}{1+\gamma\sin^2\theta}}\frac{\pi}{\sqrt{1+\gamma}}\frac{L}{d}\frac{V}{V_c}\frac{C}{C_\perp} \tag{5}$$

Solving these two equations allows to determine the ratio $C/C_\perp$ as a function of V/V_c provided that κ, γ and the ratio L/d are known.

If θ is small, expanding the two previous equations in power series of $\sin\theta$ yields [27]

$$\frac{C}{C_\perp} = \frac{1+\gamma}{1-2\gamma\frac{L}{d}} - \frac{2}{\pi}\frac{\gamma\sqrt{1+\gamma}}{1-2\gamma\frac{L}{d}}I\frac{V_c}{V} \tag{6}$$

where $I \equiv \int_0^1\sqrt{\frac{1+\kappa x^2}{1+\gamma x^2}}\mathrm{d}x$. This equation is valid as long as $\frac{2}{3}(\kappa-\gamma)\sin^3\theta \ll I$, i.e. as long as $\sin^3\theta \ll 1$ knowing that I and $\kappa-\gamma$ are usually of order unity experimentally. This imposes that the voltage is not too large, typically less than voltage $V_{\max}$ defined in the introduction by taking $\theta < 0.2$ rad. Note that these equations can also be applied to homeotropic samples by exchanging $\varepsilon_\parallel$ and $\varepsilon_\perp$ and K_1 and K_3 and by denoting by θ the angle between the director and the normal to the plates [28].

To summarize, the theory predicts that the reduced capacitance $\overline{C} = C/C_\perp$ must vary linearly as a function of the inverse of the reduced voltage $\overline{V} = V/V_c$ provided that $V_1 < V < V_2$ as in the YvS or RV models.

This calculation thus predicts that fitting with a line the capacitance curve $\overline{C}(1/\overline{V})$ in any voltage range (V_1, V_2) satisfying $V_1 > V_{\min}$ and $V_2 < V_{\max}$ should allow to determine L and the elastic anisotropy κ provided that d, $C_\perp$, V_c and the dielectric anisotropy γ are known precisely. Indeed, the value at the origin of the regression line gives L/d while its slope gives I and thus κ knowing γ.

In the following, I show that this method, as the YvS or the RV method, fails to work for measuring L and I explain why. I then show how to improve the fit procedure to obtain a reliable value of L.

3. Experimental results

3.1. Sample preparation and experimental setup

The LC chosen is 8CB. It was purchased from Synthon (Germany) and used without further purification. I measured the transition temperatures $T_{\mathrm{NA}} = 33.8°\mathrm{C}$ and $T_{\mathrm{NI}} = 40.75°\mathrm{C}$. All the samples were prepared between two ITO coated glass plates. A thin band of ITO was removed on the sides of the plates and the metallic wires used to measure the capacitance were soldered on the ITO surface with an ultrasonic iron in order to decrease the parasitic capacitances. Nickel wires were used as a spacer to fix the sample thickness and a slow-cure epoxy glue was used to bond them together. To reduce the uncertainties, thin samples ($d \approx 7.5\,\mu$m) with large surface area ($S \approx 2.5$ cm^2) were used to measure the dielectric constants, while a thick sample ($d \approx 50\ \mu$m) was used to measure V_c. In all samples, a special care was taken to the parallelism between the two glass plates, always better than $5\ 10^{-5}$ rad. The thickness of the empty cells was measured with an Ocean Optics USB2000 spectrometer. The dielectric constant $\varepsilon_\perp$ was measured using homeotropic

Preprints (www.preprints.org) | NOT PEER-REVIEWED | Posted: 14 July 2021 doi:10.20944/preprints202107.0318.v1

samples. In that case, the glass plates were treated with the polyimide Nissan SE-4811. The polyimide was deposited by spin-coating and the plates were then baked at 180°C for 30 min. The measurements of $\varepsilon_{\parallel}$ and L were performed using planar samples. The unidirectional planar anchoring was achieved by photoalignment by using a commercial azo-dye, Brilliant Yellow, sold by Sigma. The dye was dissolved in DMS (0.3 % by weight) and then deposited by spin-coating at 2000 rpm during 30 s. Before that, the plates were cleaned with sulfochromic acid, flushed with distilled water and dried at 100°C during 15 min. Once the dye was deposited, the plates were baked at 95°C for 30 min. The unidirectional planar anchoring was obtained by illuminating the plates during 30 min under normal incidence with the linearly polarized parallel light beam of a mercury vapor lamp equipped with a filter at $\lambda = 436$ nm. The power of the light beam was 1.1 mW/cm^2 so that the exposure dose was close to 2 J/cm^2. The relative humidity in the room, which is another important parameter according to Wang *et. al.* [29], was close to 40% during all the steps of preparation of the sample. With this protocole a strong planar anchoring was obtained, with no pretilt angle. All the capacitance measurements were performed at 5 kHz in the dielectric regime of the LC (I measured a charge relaxation frequency close to 500 Hz in 8CB) with a LCR meter HP 4284A, initially calibrated with standard capacitors. All the cells were filled by capillarity in the isotropic phase. Finally, the sample were placed into a home-made oven regulated to within ± 2 mK thanks to a PID controller ATNE ATSR 100.

3.2. Measurement of the dielectric constants $\varepsilon_{\parallel}$ and $\varepsilon_{\perp}$

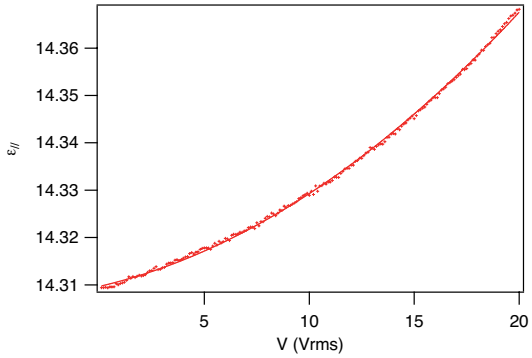

Figure 1. Dielectric constant $\varepsilon_{\parallel}$ measured in a homeotropic sample as a function of the applied voltage. The crosses are experimental points and the curve in solid line is the best fit with a parabola. $T = 35$°C.

Preprints (www.preprints.org) | NOT PEER-REVIEWED | Posted: 14 July 2021 doi:10.20944/preprints202107.0318.v1

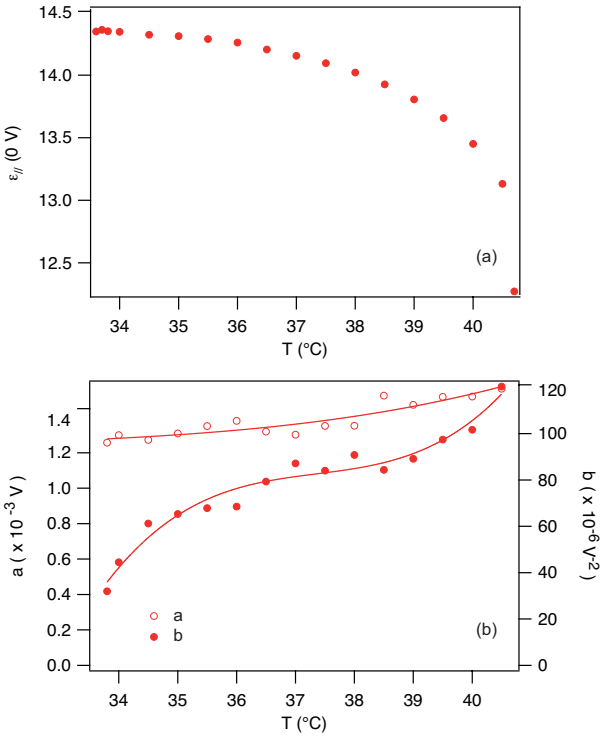

Figure 2. Variation as a function of temperature of the dielectric constant $\varepsilon_{\parallel}(0)$ extrapolated at zero voltage (**a**) and of the fit parameters a and b (**b**). The solid lines are just guides for the eye.

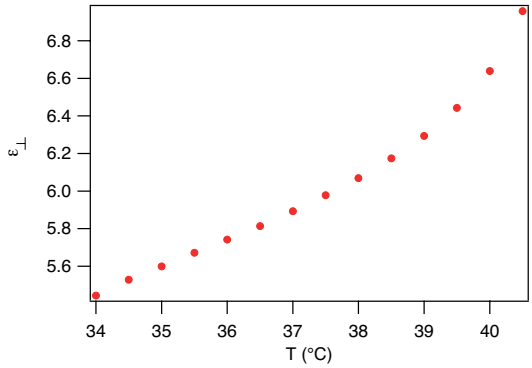

Figure 3. Dielectric constant $\varepsilon_{\parallel}$ measured below the onset of instability in a planar sample of thickness $d = 7.5\ \mu$m.

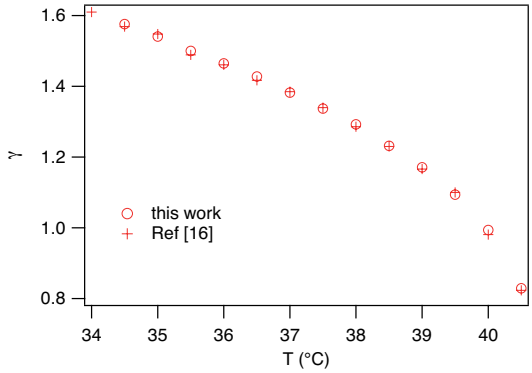

Figure 4. Dielectric anisotropy γ calculated by taking the value of $\varepsilon_{\parallel}$ extrapolated at $V = 0\ V$. The agreement with the measurements of Morris *et. al.* [30] is excellent.

Preprints (www.preprints.org) | NOT PEER-REVIEWED | Posted: 14 July 2021 doi:10.20944/preprints202107.0318.v1

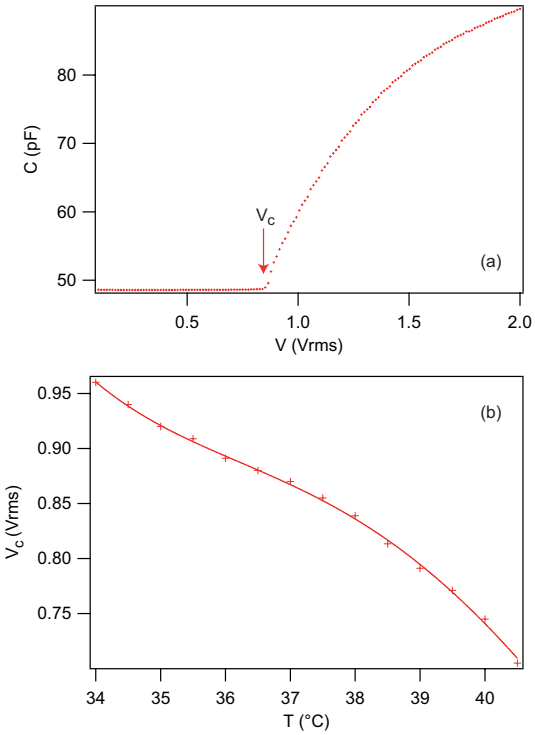

Figure 5. (**a**) Capacitance curve measured in a planar sample of thickness $d = 50$ μm at $T = 38°$C. (**b**) Critical voltage as a function of temperature. The solid line is just a guide for the eye.

I first measured the two dielectric constants. In usual experiments $\varepsilon_\perp$ is obtained by measuring the capacitance $C_\perp$ of a planar sample below the onset of Fredericksz instability and $\varepsilon_\parallel$ is deduced from an extrapolation to 0 of the capacitance curve $C(1/V)$ by assuming that $L/d \ll 1$. This requires to use very thick samples (except if the anchoring is very strong, which we do not know *a priori*) and, in that case, the capacitance measurements are less precise.

To avoid this difficulty, I directly measured $\epsilon_\parallel$ using a thin homeotropic sample of thickness $d = 7.5$ μm. Measurement were performed between 0.1 and 20 Vrms by step of 0.1 Vrms and 2 s per step. The dielectric constant $\epsilon_\perp$ was obtained by dividing the measured capacitance by the capacitance of the empty cell measured at the same voltage. In this way, I noted that $\epsilon_\parallel$ was not strictly constant, but increased slightly when the electric field was increased (Fig. 1). This phenomenon is well known and is due to two effects. The first one is due to a freezing of the director fluctuation modes and leads to a linear increase of $\epsilon_\parallel$ with the electric field [31]. The second is the Kerr effect which is microscopic in origin. It leads to a quadratic increase of the quadrupolar parameter order [32] and thus of $\epsilon_\parallel$ as a function of the electric field. This behavior is well verified in my experiments as shown in Fig. 1. In this example the experimental data are well fitted by a law of the form $\epsilon_\parallel(0) + aE + bE^2$ [33]. The same behavior is observed at all temperatures. The temperature dependence of $\epsilon_\parallel(0)$ and of the fit coefficients a and b is shown in Fig. 2.

Measurements of $\varepsilon_\perp$ was performed using a planar cell of thickness $d = 7.5$ μm. In that case, only measurements at low voltage, below V_c, are possible. In this range of voltage, I observed that the capacitance was perfectly constant, meaning that the pretilt angle was indeed equal to 0. The temperature dependence of $\varepsilon_\perp$ is shown in Fig. 3. From these measurements, I calculated γ by taken for $\varepsilon_\parallel$ the value $\epsilon_\parallel(0)$ measured at low voltage. The values calculated in this limit are in very good agreement with those measured by Morris *et. al.* [30] in a thick planar sample of thickness $d = 75$ μm (Fig. 4).

Preprints (www.preprints.org) | NOT PEER-REVIEWED | Posted: 14 July 2021 doi:10.20944/preprints202107.0318.v1

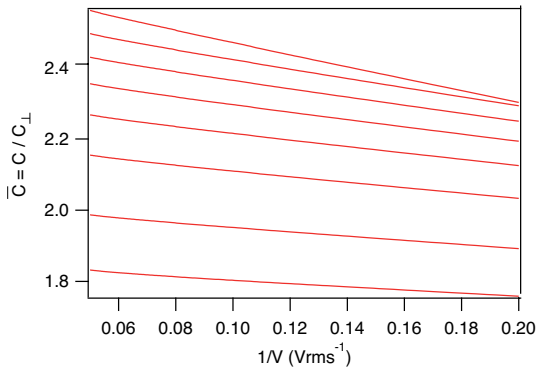

Figure 6. Reduced capacitance curves measured in a planar sample of thickness $d = 8.2$ μm at different temperatures. From top to bottom, $T = 34, 35, 36, 37, 38, 39, 40$ and $40.5°$C.

3.3. Measurement of the critical voltage V_c

The critical voltage was measured with a 50 μm-thick sample. With this thickness, the measured voltage V_c' is equal to V_c to better than 1% if $L < 0.25$ μm, a condition well fulfilled experimentally in my experiments at all temperature, as I will check *a posteriori* (see Fig. 10(a) below). The measurements were performed by increasing very slowly the voltage by increments of 10 mV with a time interval of 30 s between each increment. A capacitance curve is shown in Fig. 5 (**a**). This curve shows that the measured capacitance is perfectly constant below the onset of instability, showing that there is no pretilt in my sample. The measured critical voltage as a function of temperature is shown in Fig. 5 (**b**).

3.4. Measurements of the extrapolation length L

As the anchoring is expected to be strong with Brilliant Yellow, a pretty thin sample must be used in order that the tilt angle θ on the plates deviates from 0 in a measurable way under the action of the electric field. For this reason, I used a 8.3 μm-thick sample and I measured the capacitance between 0.1 V and 0.5 Vrms typically to obtain $C_\perp$ and between 5 and 20 Vrms to measure the extrapolation length L. At voltage V=5 Vrms the condition $V > 6V_c$ is always satisfied, so that the basic equations (4) and (5) apply. Typical curves $\overline{C}(\overline{V})$ measured between 5 and 20 Vrms are shown in Fig. 6. These curves are almost linear, suggesting that angle θ remains small and Equation (6) applies. In that case, fitting the curves with the linear law $1 + \gamma_{app} - p\,\overline{V}$ in any voltage range (V_1, V_2) with $V_1 > 5$ Vrms and $V_2 < 20$ Vrms should allow me to measure L by using the equation

$$\frac{L}{d} = \frac{\gamma_{app} - \gamma}{2\gamma(1 + \gamma_{app})} \tag{7}$$

derived from Equation (6) and the value of γ given in Fig. 3. To test this method, I fitted the curves within different intervals of voltage (V_1, V_2). For each fit, I calculated L and $V_{\max}$ by using the formula given in the introduction to check whether $V_2 < V_{\max}$ in order that the model applies. In principe, all the measurements should coincide if the model applies. In practice, it is not at all the case, the value of L crucially depending on the choice of the interval (V_1, V_2), even when the model is *a priori* valid, as the reader can see in Table 1 obtained by fitting the curve at $T = 35°$C. To summarize, I met the same difficulties as Nastishin *et al.* when they used the YvS or RV method. In a similar way, I also noted that the larger V_2, the larger the value of L found from the linear fit.

Preprints (www.preprints.org) | NOT PEER-REVIEWED | Posted: 14 July 2021 doi:10.20944/preprints202107.0318.v1

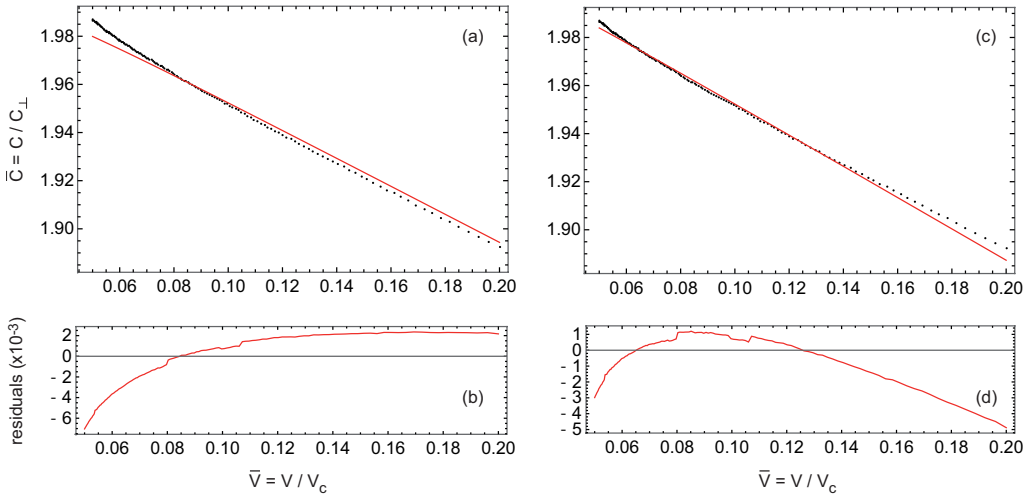

Figure 7. Capacitance curve measured at $T = 40°C$ (the dots are the experimental points) and its fits (solid lines) calculated by taking $\kappa = -0.08$ and $L = 0.045$ μm (a,b) or $\kappa = 0.72$ and $L = 0.05$ μm. Here $\varepsilon_{\parallel}$ is assumed to be constant, equal to $\varepsilon_{\parallel}(0)$.

Table 1

Voltage range (V_1, V_2)	**Fitted value of** L **(in** μ**m)**	V_2	**Is the model applicable?**
(5 V, 9 V)	0.0104	29 V	Yes
(5 V, 13 V)	0.0144	21 V	Yes
(5 V, 17 V)	0.0178	17 V	Yes
(5 V, 20 V)	0.0202	15 V	No

In their paper, Nastishin *et al.* [17] suggest that this problem could be due to inhomogeneities of the anchoring conditions. I do not share that view, at least in my experiments, and suggest that the problem is rather due to the approximations done by using Eq. (6) with $\varepsilon_{\parallel}$ constant.

For this reason, I tried in a first attempt to fit my experimental curves with the full equations (4) and (5), while still keeping $\varepsilon_{\parallel}$ constant, equal to $\varepsilon_{\parallel}(0)$. In that case, there are two fit parameters: the elastic anisotropy κ that essentially fixes the slope of the curve and the ratio L/d that fixes the "height" of the curve. Surprisingly, I noted that it was not possible to fit correctly my experimental curves at large voltages even with the full equations. The graphical comparison between the experimental curve and the calculated ones for two particular values of κ is shown in Fig. 7. For each fit, the root-mean-square deviation between the experimental curve and the fit curve is minimized as a function of L. In this example, $T = 40°C$ and the expected value for κ at this temperature is close to -0.08 according to previous measurements performed in thick samples at low voltage when the anchoring energy can be assumed to be infinite [30] or by using a full-optical method [24]. For this reason, I performed the first fit (Fig. 7**a**-**b**) with this value and found $L = 0.037$ μm. In that case, the slope of the theoretical curve is correct at low voltage (below 10 Vrms), but the model fails to reproduce the increase of the capacitance at large voltage, above 10 V. Increasing the value of κ allows to better fit the behavior at large voltage, but this time, the slope of the theoretical curve is clearly too large at low voltage. The best global fit is obtained by taking $\kappa = 0.72$ (which is very different from the expected value -0.08) and $L = 0.05$ μm and is shown in Fig. 7(**c**-**d**). This analysis shows the impossibility to reasonably fit the experimental curve in the whole range of voltages used experimentally. Something is clearly missing in the model.

Preprints (www.preprints.org) | NOT PEER-REVIEWED | Posted: 14 July 2021 doi:10.20944/preprints202107.0318.v1

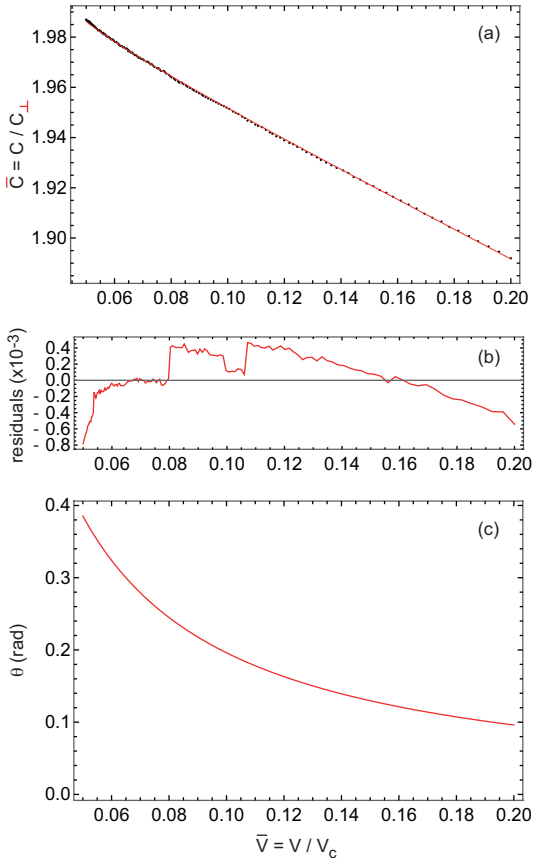

Figure 8. (a) Capacitance curve measured at $T = 40°C$ (the dots are the experimental points) and its fit (in solid line) obtained by taking into account the variation with electric field of $\varepsilon_{\|}$. The best fit is obtained by taking $\kappa = -0.08$ and $L = 0.0293$ μm. (b) Residuals. (c) Angle θ on the plates as a function of the voltage.

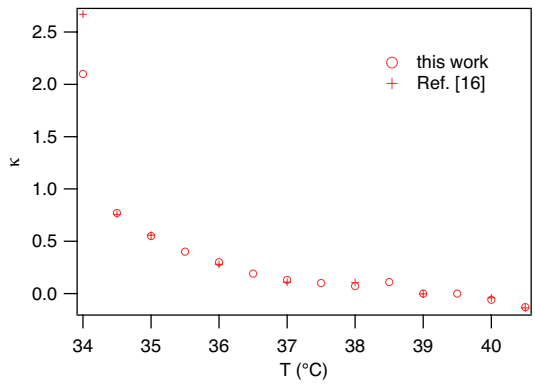

Figure 9. Values of κ obtained from the fit of the capacitance curves shown in Fig. 6 by taken into account the electric field variation of $\varepsilon_{\|}$. The agreement with the values given by Morris *et. al.* is excellent.

Preprints (www.preprints.org) | NOT PEER-REVIEWED | Posted: 14 July 2021 doi:10.20944/preprints202107.0318.v1

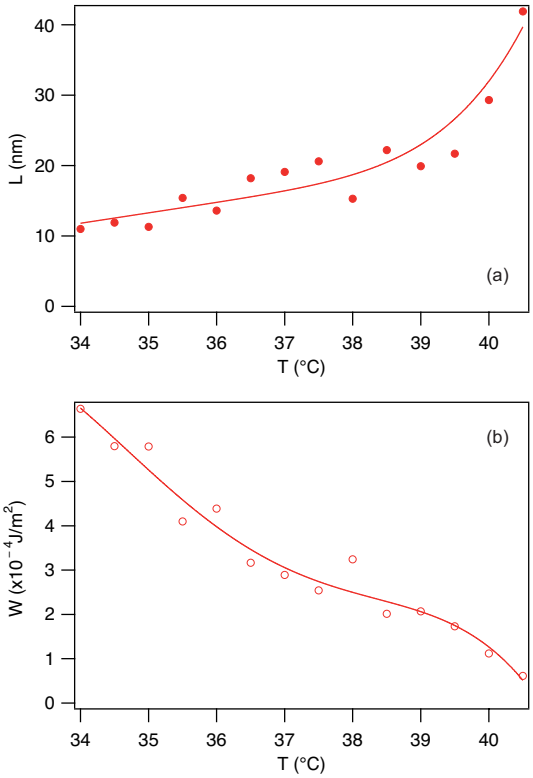

Figure 10. (a)Values of L obtained from the fit of the capacitance curves shown in Fig. 6 by taken into account the electric field variation of $\varepsilon_{\|}$. (b) Corresponding values of W.

For this reason, I tried to fit again my curves by taking into account the dependence with the electric field of the dielectric constant $\varepsilon_{\|}$ measured previously in homeotropic samples (Fig. 2). This correction is here justified because the sample is almost homeotropic between 5 and 20 Vrms and was already taken into account by Murauski *et al.* [27] in a similar problem. With the aid of Mathematica 12, I realized that it was possible to considerably improve the quality of the fits. The example of the same curve as before measured at $T = 40°$C is shown in Fig. 8. In this case the best fit as a function of κ and L of the whole curve gives $\kappa = -0.08$ and $L = 0.0293$ μm with a residual always less than $5\ 10^{-4}$ in spite of the fact that angle θ is pretty large at this temperature at large voltage. This is ten times better than before, as we can see by comparing the residuals of the fits shown in Figs. 7 and 8. In addition, the value of κ found here is in very good agreement with that found by Morris *et. al.* [30] or by us (I and J. Colombier) by using a full-optical method [24]. This good agreement was confirmed at all the other temperatures, showing the importance of taking into account the electric field dependence of $\varepsilon_{\|}$ in the fit of the experimental curves at large electric field. The values of κ and L obtained in this way are shown in Fig. 9 and 10(**a**), respectively. Finally, the last graph in Fig. 10(**b**) shows the temperature dependence of the anchoring energy W calculated by using the value of K_1 deduced from our measurements of V_c by taking $\varepsilon_a = \varepsilon_{\|}(0) - \varepsilon_{\perp}$. The graph shows that W decreases when the temperature increases and approaches the melting temperature. By contrast, no divergence is observed in the vicinity of the smectic A phase, contrary to what is observed for the bend and twist elastic constants.

4. Role of flexoelectric effects

As we can see in Fig. 8, the fit is not perfect. For this reason I tried to improve it by introducing a flexoelectric contribution following a procedure detailed in a previous publication [24]. I found that the best fits were systematically obtained by taking the bulk flexoelectric coefficient $e^{\star} = 0$ [34]. That means that flexoelectric effects are completely screened out by the ions in the present experiments. This result was expected because the

Preprints (www.preprints.org) | NOT PEER-REVIEWED | Posted: 14 July 2021 doi:10.20944/preprints202107.0318.v1

Debye length L_D in our samples is of the order of 50 nm, which is indeed much smaller than the sample thickness [35–37]. This value was obtained from the measurement of the charge relaxation frequency $f_c \approx 500\,\text{Hz}$ by using formula $\lambda_D \approx \sqrt{\frac{D}{2\pi f_c}}$ [38] and by taking $D = 10\,\mu\text{m}^2/\text{s}$ for typical value of the diffusion coefficient of ions in 8CB [39].

5. About the Rapini-Papoular form of the anchoring energy

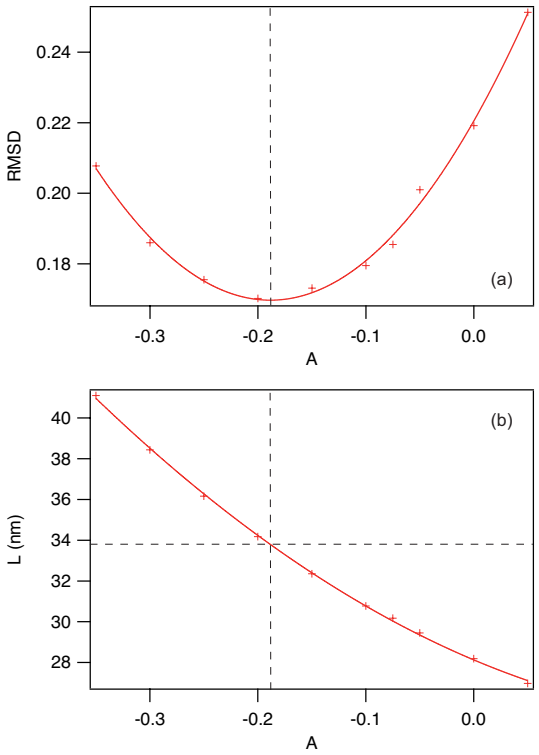

Figure 11. (a)RMSD as a function of A for the experimental curve measured at $T = 40°\text{C}$. (b) Value of L that minimizes the RMSD as a function of A.

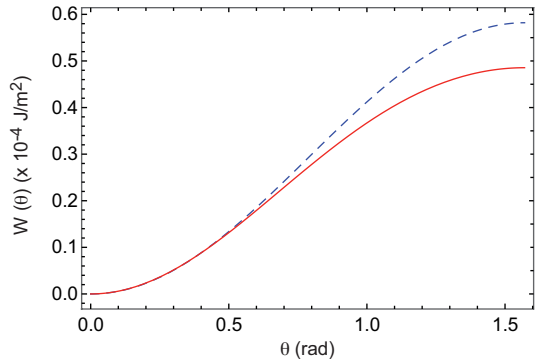

Figure 12. Comparison between the best Rapini-Papoular potential (curve in blue dashed line) and the best modified Rapini-Papoular potential (curve in red solid line). The two potentials are almost indistinguishable below $\theta = 0.4$ rad, meaning that in our experiment the Rapini-Papoular potential can be used to fit the data.

Numerous experiments suggest that the actual anchoring potential shifts from the Rapini-Papoular form at large tilt angle [2,3,15,40–43]. Another possibility to improve the quality of the fits is to modify the form of the anchoring potential. Several solutions have been proposed in the literature. One of them consists of replacing the sinus in the Rapini-Papoular potential by an elliptic sinus [42]. This function is complicated to work

Preprints (www.preprints.org) | NOT PEER-REVIEWED | Posted: 14 July 2021 doi:10.20944/preprints202107.0318.v1

with and I did not use it. Another much simpler and very classical solution is to add a term in $\sin^4\theta$ to the potential [15,40,41,44,45]. In that case the anchoring potential can be written in the form

$$W(\theta) = \frac{1}{2} W \frac{\sin^2\theta + A\sin^4\theta}{1+A} \tag{8}$$

and the torque equation (5) becomes

$$\frac{1+2A\sin^2\theta}{1+A}\sin\theta = \sqrt{\frac{1+\kappa\sin^2\theta}{1+\gamma\sin^2\theta}}\frac{\pi}{\sqrt{1+\gamma}}\frac{L}{d}\frac{V}{V_c}\frac{C}{C_\perp} \tag{9}$$

To test the pertinency of this correction, I fitted the capacitance curve measured at 40°C with this new potential by using the value of κ previously found and I minimized the root-mean-square deviation (RMSD) between the experimental curve and the theoretical curve obtained by solving numerically with Mathematica Equations (4) and (9). In practice, the RMSD was minimized as a function of $L = K_1/W$ for different values of A. The result is shown in Fig. 11. This graph shows that the RMSD passes through a minimum for $A = -0.188$ and $L = 33.8$ nm.

This calculation shows that the actual potential is different from the Rapini-Papoular potential and flattens when $\theta \to \pi/2$. Such a tendency was already observed experimentally [14,15]. The difference between this potential and the one of the Rapini-Papoular form is nonetheless very small in the range of angles θ probed in this experiment ($\theta < 0.4$ rad according to Fig. 8(**c**) as the reader can see in Fig. 12. This explains why the RMSD does not change much as a function of A in Fig. 11(**a**). In practice, it would interesting to use larger field to test the relevance of this correction to the Rapini-Papoular potential. I also mention that this value of A is compatible with the second order character of the Fredericksz transition observed here as shown by Guochen *et al.* [46].

6. Conclusions

This analysis confirms that neglecting the dependence on the electric field of the dielectric constant $\varepsilon_\parallel$ in the analysis of the capacitance curves at high voltage may be dangerous and lead to wrong values of the extrapolation length [27]. This effect is clearly at the origin of the breakdown of the analysis of the capacitance curves with the linear law given in Eq. (6) which gives values of L strongly dependent on the voltage range used to fit the data when $\varepsilon_\parallel$ is taken constant. I note that the behavior observed in my analysis, namely a value L that systematically decreases when the fits are done at large voltages, is the same as the one reported by Nastishin et. al. [5] by using the YvS or the RV techniques. This result suggests that the problems faced by these authors are due to the variation with the electric field of the dielectric constant $\varepsilon_\parallel$ rather than to anchoring inhomogeneities in the samples. This effect should be particularly important in LC such as 8CB which is composed of molecules with a strong electric dipole moment.

To measure the extrapolation length, I thus propose a new procedure that is more general than that proposed by Murauski *et al.* [27] and perhaps easier to implement. This procedure consists of solving directly the full equations (3) and (4) governing the problem, which is much more rigorous than using the approximate equation (5) as these authors do. Indeed, this equation assumes that the anchoring angle θ is small, typically less than 0.2 rad, which is a strong limitation at large field [1]. Another advantage of my method is that it gives simultaneously the values of the two dielectric constants and of the elastic constants K_1 and K_3. My method can also be used to test the shape of the anchoring potential, as it does not assume that the anchoring potential is of the Rapini-Papoular form. This method is also easy to implement because the equations (3) and (4) are easily solved numerically, for instance with Mathematica.

[1] I also mention here that formula (2) in Ref. [10] is wrong and must be read $B = \sqrt{\frac{(1-y_p)(1+\kappa y_p)}{1+\gamma y_p}}$

Last but not least, this method can also be generalized to the case of samples with a pretilt angle, as the ones obtained by using a rubbed polymer. In that case, it is sufficient to replace θ by $\theta - \theta_a$ in the l.h.s. of Equation (5) where θ_a is the pretilt angle. Note also that the measurement of V_c must be performed with a thick *parallel* planar sample (the reason for this is explained in Ref. [24]). This is important because badly measuring V_c changes the slope of the experimental curves $\overline{C}(\overline{V})$ and thus the value of κ. By contrast, the measurements of the extrapolation length must be performed with an *antiparallel* sample in order that Equations (3) and (4) (or (9)) apply. This method could also be applied to LC with a negative dielectric anisotropy to measure the polar anchoring energy under homeotropic anchoring.

In the future it would be interesting to perform experiments at larger field to better test the validity of the Rapini-Papoular form of the anchoring potential. It would also be interesting to compare the values of L and A obtained in this way with those obtained, for instance, by measuring the critical voltage V_c' in a wedge sample [47] and by using more sophisticated methods as the one based on spectroscopic ellipsometry [48,49] or the all-optical compensated method of Murauski *et al.* [14].

Acknowledgments: The author warmly thanks Mohamed A. Gharbi for his invitation to submit a paper in this Special Issue of Applied Sciences, Pawel Pieranski and Guilhem Poy for useful comments, Artem Petrossyan for the loan of the ultrasonic iron and J. Ignés-Mullol for the sample of the polyimide Nissan SE-4811.

Conflicts of Interest: The author declares no conflict of interest.

References

1. Oswald, P.; Pieranski, P. *Nematic and cholesteric liquid crystals: concepts and physical properties illustrated by experiments*; CRC Press: Boca Raton, USA, 2005; pp. 339–366.
2. Jerome, B. Surface effects and anchoring in liquid crystals. *Rep Prog Phys* **1991**, *54*, pp. 391–452.
3. Jerome, B. Physical Properties: Surface Alignment. In *Handbook of Liquid Crystals: Fundamentals*; Demus D., Goodby J., Gray G.W., Spiess H.-W., Vill V. Eds; Wiley Online Library: Hoboken, USA, 1998; pp. 535–548.
4. Chen, R.H. *Liquid crystal displays: fundamental physics and technology*; John Wiley & Sons: Hoboken, USA, 2011.
5. Nastishin, Yu A.; Polak, R.D.; Shiyanovskii, S.V.; Bodnar, V.H.; Lavrentovich, O.D. Nematic polar anchoring strength measured by electric field techniques. *J. Appl. Phys.* **1999**, *86*, 4199–4213.
6. Ryschenkow, G.; Kleman, M. Surface defects and structural transitions in very low anchoring energy nematic thin films. *J. Chem. Phys.* **1976**, *64*, 404–412.
7. Riviere, D.; Levy, Y.; Guyon, E. Determination of anchoring energies from surface tilt angle measurements in a nematic liquid crystal. *J. Phys. Lett. Paris* **1979**, *40*, 215–218.
8. Barbero, G.; Barberi, R. Critical thickness of a hybrid aligned nematic liquid crystal cell. *J. Phys. Paris* **1983**, *44*, 609–616.
9. Barbero, G.; Madhusudana, N.V.; Durand, G. Weak anchoring energy and pretilt of a nematic liquid crystal. *J. Phys. Lett. Paris* **1984**, *45*, 613–619.
10. Marusii, T. Ya; Reznikov, Yu A.; Reshetnyak, V. Yu; Soskin, M.S.; Khizhnyak, A.I. Scattering of light by nematic liquid crystals in cells with a finite energy of the anchoring of the director to the wails. *Sov. Phys. JETP* **1986**, *64*, 502–507.
11. Vilfan, M.; Mertelj, A.; Čopič, M. Dynamic light scattering measurements of azimuthal and zenithal anchoring of nematic liquid crystals. *Phys. Rev. E* **2002**, *65*, 041712.
12. Vilfan, M.; Čopič, M. Azimuthal and zenithal anchoring of nematic liquid crystals. *Phys. Rev. E* **2003**, *68*, 031704.
13. Subacius, D.; Pergamenshchik, V.M.; Lavrentovich, O.D. Measurement of polar anchoring coefficient for nematic cell with high pretilt angle. *Appl. Phys. Lett.* **1995**, *67*, 214–216.
14. Murauski, A.; Chigrinov, V.; Kwok, H.-S. New method for measuring polar anchoring energy of nematic liquid crystals. *Liq. Cryst.* **2009**, *36*, 779–786.
15. Yokoyama, H.; Van Sprang, H.A. A novel method for determining the anchoring energy function at a nematic liquid crystal-wall interface from director distortions at high fields. *J. Appl. Phys.* **1985**, *57*, 4520–4526.
16. Rapini, A.; Papoular, M. Distorsion d'une lamelle nématique sous champ magnétique conditions d'ancrage aux parois. *J. Phys. Coll. Paris* **1968**, *30*, C4–54.
17. Nastishin, Yu A.; Polak, R.D.; Shiyanovskii, S.V.; Lavrentovich, O.D. Determination of nematic polar anchoring from retardation versus voltage measurements. *Appl. Phys. Lett.* **1999**, *75*, 202–204.
18. Yaroshchuk, O.; Gurumurthy, H.; Chigrinov, V.G.; Kwok, H.S.; Hasebe, H.; Takatsu, H. Photoalignment properties of brilliant yellow dye. Proceedings of the International Display Workshop, Sapporo, Japan, 5-7 December 2007, 1665–1668.

19. Chigrinov, V.; Kwok, H.S.; Takada, H.; Takatsu, H. Photo-aligning by azo-dyes: physics and applications. *Liq. Cryst. Today* **2005**, *14*, 1–15.
20. Folwill, Y.; Zeitouny, Z.; Lall, J.; Zappe, H. A practical guide to versatile photoalignment of azobenzenes. *Liq. Cryst.* **2020**, *48*, 1–11.
21. Fréedericksz, V.; Zolina, V. Forces causing the orientation of an anisotropic liquid. *Trans. Far. Soc.* **1933**, *29*, 919–930.
22. Deuling, H.J. Deformation of nematic liquid crystals in an electric field. *Mol. Cryst. Liq. Cryst.* **1972**, *19*, 123–131.
23. Gruler, H.; Scheffer, T.J.; Meier, G. Elastic constants of nematic liquid crystals: I. Theory of the normal deformation. *Z. Naturforsch. A* **1972**, *27*, 966–976.
24. Oswald, P.; Colombier, J. On the measurement of the bend elastic constant in nematic liquid crystals close to the nematic-to-SmA and the nematic-to-NTB phase transitions. *Liq. Cryst.* **2021**, 1–25.
25. Uchida, T.; Takahashi, Y. New method to determine elastic constants of nematic liquid crystal from CV curve. *Mol. Cryst. Liq. Cryst.* **1981**, *72*, 133–137.
26. Toko, Y.; Akahane, T. Evaluation of pretilt angle and polar anchoring strength of amorphous alignment liquid crystal display from capacitance versus applied voltage measurement. *Mol. Cryst. Liq. Cryst. Sect. A* **2001**, *368*, 469–481.
27. Murauski, A.; Chigrinov, V.; Muravsky, A.; Yeung, Fion S.-Y.; and Ho, J.; Kwok, H.-S. Determination of liquid-crystal polar anchoring energy by electrical measurements. *Phys. Rev. E* **2005**, *71*, 061707.
28. Akiyama, H.; Iimura, Y. New measurement method of polar anchoring energy of nematic liquid crystals. *Mol. Cryst. Liq. Cryst. Sect. A* **2000**, *350*, 67–77.
29. Wang, J.; West, J.; McGinty, C.; Bryant, D.; Finnemeyer, V.; Reich, R.; Berry, S.; Clark, H.; Yaroshchuk, O.; Bos, P. Effects of Humidity and Surface on Photoalignment of Brilliant Yellow. *Liq. Cryst.* **2017**, *44*, 863–872.
30. Morris, S.W.; Palffy-Muhoray, P.; Balzarini, D.A. Measurements of the bend and splay elastic constants of octyl-cyanobiphenyl. *Mol. Cryst. Liq. Cryst.* **1986**, *139*, 263–280.
31. De Gennes, P.-G.; Prost J. *The Physics of Liquid Crystals*; Clarendon Press: Oxford, USA, 1993.
32. Lelidis, I.; Nobili, M.; Durand, G. Electric-field-induced change of the order parameter in a nematic liquid crystal. *Phys. Rev. E* **1993**, *48*, 3818-3821.
33. Basappa, G.; Madhusudana, N.V. Effect of a strong electric field on a nematogen: evidence for polar short range order. *Eur. Phys. J. B* **1998**, *1*, 179–187.
34. Prost, J.; Pershan, P.S. Flexoelectricity in nematic and smectic-A liquid crystals. *J. Appl. Phys.* **1976**, *47*, 2298–2312.
35. Dozov, I.; Barbero, G.; Palierne, J.-F., Durand, G. Nonlocal electric field and large distortions in nematic liquid crystals. *EPL* **1986**, *1*, 563–569.
36. Palierne J.-F. Elasticlike contribution of electric origin to the distortion free energy of nematics. *Phys. Rev. Lett.* **1986**, *56*, 1160-1162.
37. Smith, A.A.T.; Brown, C.V.; Mottram, N.J. Theoretical analysis of the magnetic Freedericksz transition in the presence of flexoelectricity and ionic contamination. *Phys. Rev. E* **2007**, *75*, 041704.
38. Bazant, M.Z.; Thornton, K.; Ajdari, A. Diffuse-charge dynamics in electrochemical systems. *Phys. Rev. E* **2004**, *70*, 021506.
39. Khazimullin, M.V.; Lebedev, Y.A. Influence of dielectric layers on estimates of diffusion coefficients and concentrations of ions from impedance spectroscopy. *Phys. Rev. E* **2019**, *100*, 062601.
40. Yang, K.H. On the determination of liquid crystal-to-wall anchoring anisotropy by the surface-plasmon polariton technique. *J. Appl. Phys.* **1982**, *53*, 6742–6745.
41. Yang, K.H.; Rosenblatt, C. Determination of the anisotropic potential at the nematic liquid crystal-to-wall interface. *Appl. Phys. Lett.* **1983**, *43*, 62–64.
42. Barnik, M.I.; Blinov, L.M.; Korkishko, T.V.; Umansky, B.A.; Chigrinov, V.G. Investigation of NLC director orientational deformations in electric field for different boundary conditions. *Mol. Cryst. Liq. Cryst.* **1983**, *99*, 53–79.
43. Barbero, G.; Madhusudana, N.V.; Palierne, J.-F.; Durand, G. Optical determination of large distortion surface anchoring torques in a nematic liquid crystal. *Phys. Lett. A* **1984**, *103*, 385–388.
44. Barbero, G.; Durand, G. On the validity of the Rapini-Papoular surface anchoring energy form in nematic liquid crystals. *J. Phys. Paris* **1986**, *47*, 2129–2134.
45. Alexe-Ionescu, A.L.; Barbero, G.; Gabbasova, Z.; Sayko, G.; Zvezdin, A.K. Stochastic contribution to the anchoring energy: Deviation from the Rapini-Papoular expression. *Phys. Rev. E* **1994**, *49*, 5354–5358.
46. Guochen, Y.; Jianru, S.; Ying, L. Surface anchoring energy and the first order Freedericksz transition of a NLC cell. *Liq. Cryst.* **2000**, *27*, 875–882.
47. Gu, D.-F.; Uran, S.; Rosenblatt, C. A simple and reliable method for measuring the liquid crystal anchoring strength coefficient. *Liq. Cryst.* **1995**, *19*, 427–431.
48. Hirosawa, I. Method of characterizing rubbed polyimide film for liquid crystal display devices using reflection ellipsometry. *Jap. J. Appl. Phys.* **1996**, *35*, 5873.
49. Marino, A.; Tkachenko, V.; Santamato, E.; Bennis, N.; Quintana, X.; Otón, J.M.; Abbate, G. Measuring liquid crystal anchoring energy strength by spectroscopic ellipsometry. *J. Appl. Phys.* **2010**, *107*, 073109.